Accelerated aging tests and characterizations of solar mirrors: Comparison of combinations of stress factors on degradation

Antoine Grosjean, Estelle Le Baron, Anne-Claire Pescheux, Angela Disdier

Accelerated Aging Tests and Characterizations of Solar Mirrors: Comparison of Combinations of Stress Factors on Degradation

Antoine Grosjean[1], Estelle Le Baron[1*], Anne-Claire Pescheux[1], Angela Disdier[1]

[1] *Univ. Grenoble Alpes, CEA-LITEN, DTBH, F-73375 Le Bourget du Lac, France*

[*] *Corresponding author: estelle.lebaron@cea.fr*

Abstract. Solar mirrors for concentrated solar power (CSP) plants are expected to ensure a proper efficiency during 30 years. Due to this long time, accelerated aging tests of solar materials are crucial to estimate the real degradation in-service. However, most publications in the CSP field are based on standardized tests which are not sufficient to reach the durability of products in service on all CSP sites and all the market. The impacts on the material properties of unitary stress factors such as temperature, irradiation and humidity have been studied, and models have been proposed for different kinds of materials. All of these models include one or two stress factors, various magnitudes doses, and material dependent parameters. This study aimed to compare degradation under multifactor of stresses: temperature, humidity and irradiation on solar mirrors, with a focus on verification of two following hypotheses:

1. the coupling hypothesis based on the multiplication of the acceleration factors without synergy between themselves,
2. the initialization hypothesis for these three stress factors where the order of application of these tests does not matter.

This last hypothesis was never formulated in the models but it is studied in this article. In this paper, we present the results of four different silvered glass mirrors subjected to several accelerated aging tests. The conclusion of this work will help the manufacturer to compare their technology to the others and to ensure the reproducibility of aging between indoor chambers and outdoor sites.

Keywords: CSP plants, Solar mirrors, Accelerated aging test, Solar reflectance.

Nomenclature

B, C : Constants
Ea : Activation energy, in $J \cdot mol^{-1}$
T : Temperature, in K
DNI : Direct Normal Irradiation, in $W \cdot m^{-2}$
Irr : Irradiation, in $W \cdot m^{-2}$
p : Schwarschild's coefficient
R : Perfect gas constant, in $J \cdot mol^{-1} \cdot K^{-1}$
R_D : loss of specular reflectance in the Lee equation, no unit
t: Index for test
t(s) : time
s : Index for site
HMI : Hydrargyrum Medium-arc Iodide
RH : Relative humidity, in %
IS : Integrating Sphere
D&S : 15R-USB Reflectometer from D&S
A : Global acceleration factor
α : Individual acceleration factor or risk factor
β : Humidity activation energy

γ : Frequency factor, in h^{-1} $\bar{x}$: Average of x σ : Standard deviation

1. Introduction

Concentrated solar power (CSP) can produce carbon dioxide-free and renewable energy in which sunlight is concentrated by mirrors on an absorber that heats a fluid. Different kinds of CSP technologies are available today and their main advantages cooperate with other technologies which are in the presence of a thermal storage [1]. The Requirement for CSP plants to produce electrical energy nearly 24h/24h creates the obligation to have a huge solar field, for producing during sun hours enough energy to supply the power block during night hours [2], [3]. This explains why the solar field is an important part of the total investment. Indeed, solar field represents around 30% of the installed cost of a CSP plant [4]. It is made of linear (parabolic trough or Fresnel) or punctual (tower or dish) thermal absorbers with reflectors to focus the sun light. Durability of solar mirrors is a key point in CSP plants because they represent an important investment, with significant payback time. Concerning solar mirrors, a lifetime of 30 years is regularly cited in the bibliography [5], [6]. Being able to predict the aging and the degradation rate of solar mirrors can be profitable to many points:

- To correctly calculate the energy produced over time and to deduce more squarely the plant LCOE [7].
- To help scientific and industrial companies to produce best quality of mirrors by identifying the key factors of degradation [7].
- To reassure banks and investors. Predicting more accurately future events such as the replacement of mirrors will make CSP plants less risky investments. This point is not negligible, as the risk factor of investment conditions interest rates [8].

A significant problem with earlier plants was broken/cracked mirrors or mirrors separating from their pads, with most of this damage coming from the effects of wind loads [9]. This led to loss of reflectance, accounting for a fifth of all lost power production outages, so the costs are higher than just the O&M costs to fix or repair the mirrors [10]. Reducing the rate of breakage and loss of reflectance can therefore help to reduce costs significantly. In this paper, an extensive test campaign of accelerated aging tests has been performed with monolithic silvered-glass mirrors from several manufacturers to compare them. The accelerated aging tests were conducted for an extended period in order to determine the testing time when there is appearance of significant degradation of mirrors. We analyzed how to mix several predominant factors that can be involved in the solar mirror degradation and how modeling the coupling of these factors are discussed.

2. Theoretical Background

2.1. Theoretical lifetime models with one stress factor

Different reviews of accelerated ageing test exist in the literature [11–13]. Recently C. Avenel et al. have written a review of models and their application to solar mirror of CSP plants [14]. This paper presents shortly the mathematical models with one stress factor (the temperature, the irradiation or the humidity) or coupling several stress factors combining humidity and temperature details under.

2.1.1. Temperature

In all durability fields, temperature is the most studied stress factor. Indeed, a high temperature accelerates the material degradation because the kinetics of chemical processes vary with temperature. The temperature has the double effect to increase the probability of contacts between molecules and to change the material mechanical behavior. The most effective law for degradation due to the temperature stress factors is the Arrhenius relationship [11], [12], [15]. This law assumes that a chemical degradation process is controlled by a reaction rate constant , noted k [16]. This constant is due to two different factors which define a specific product or material, noted γ for the frequency factor (in h^{-1}) and Ea for the activation energy ($J \cdot mol^{-1}$). Finally, the reaction rate constant k is also a function of temperature (T, in K) and R Boltzmann's constant (or the universal gas constant, depending of Ea unit).

$$k = \gamma \cdot exp(\frac{-Ea}{R \cdot T}) \quad (1)$$

For solar mirror, the temperature of use is the local temperature in the solar field on one site, noted here T_s. T_t is the test temperature during the accelerated test where $T_t >> T_s$. The acceleration factor a_T calculated from the previous law is given by the following equation (2) [13]:

$$a_T = exp(\frac{-Ea}{R}\left[\frac{1}{T_t} - \frac{1}{T_s}\right]) \quad (2)$$

2.1.2. Irradiation

Degradation due to light irradiation is usually called photo-degradation. The impact of light, particularly the impact of short wavelength such as UV (280-400 nm) on the properties of organic materials has been studied in numerous studies [17–20]. This is mainly due to the capacity of UV to interact with several chemical connections, particularly the connections between carbon, oxygen or hydrogen. For solar mirrors we should consider the UV flux density and the total irradiation flux density, as solar mirrors are obviously installed in area with important DNI, up to 2000 kWh/m^2·y (7.2e+9 J / year) [21]. The fundamental law used for aging by irradiation is the reciprocity law, which makes it possible to calculate an energetic dose of radiation received, therefore in joules (J). This law stipulates that the same dose (in J) of light causes the same degradation effects. However, many experimental results have clearly shown deviations from this law. The equation (3) takes into account a Schwarzschild coefficient, noted p, to link power and time more efficiently [22], [23]. The irradiation acceleration factor α_T is given by the following formula, with I_t the test irradiation and I_s the irradiation on the site as a function of the Schwarzschild's coefficient (p), depending on the material [20], [24].

$$a_T = (\frac{I_t}{I_s})^p \quad (3)$$

Previous studies have shown that three different radiative test aging chambers (Sepap, Suntest and UV-5X) produce different results of the same studied solar mirrors [20]. The different spectral irradiations (in W/m^{2}nm^{-1}) for each chamber due to different lamps is strongly suspected. To avoid this conflict, we have performed our tests with the same light source (HMI) in the same climatic chamber UV-5X.

2.1.3. Humidity

Moisture is still described as one of the predominant ageing mechanism. In the case of mirrors, it promotes corrosion of the reflective layer, degrades the paint layers of monolithic mirrors and the inorganic surface layers of first surface mirrors (aluminum and polymer) [25]. Several approaches exist for modeling the moisture. We will briefly detail the two models: the Eyring's law and the Peck's model [11], [14].

Eyring models

Two models have been developed based on Eyring's law. The time from which the performance criterion is reached is a function of an activation energy for temperature (noted *Ea*) and an activation energy for humidity (noted β). The latter is also sometimes referred to the Eyring coefficients. There is therefore a strong similarity with Arrhenius' law for temperature [14]. In the end, the acceleration factor α_{RH} is a function of temperature, and humidity according to stress conditions between the site (noted index s) and the aging test noted index t) is written [26]:

$$a_{T,RH} = exp(\frac{E_a}{R}\left[\frac{1}{T_s} - \frac{1}{T_t}\right] + \beta\left[\frac{1}{RH_s} - \frac{1}{RH_t}\right]) \quad (5)$$

Peck model

This model is well accepted in the community and is generally referred to the "Peck model" [27]. Peck model was established by the epoxy packaging of microelectronic systems and corresponds to the following equation (6). The effect of humidity is expressed as the ratio between the relative humidity of the site (RH_s) and the test relative humidity (RH_t) where the material-dependent constant n replaces the Eyring coefficient β used previously.

$$a_{RH} = (\frac{RH_s}{RH_t})^n \cdot exp(\frac{E_a}{R}\left[\frac{1}{T_s} - \frac{1}{T_t}\right]) \quad (6)$$

2.2. Theoretical models of coupling several accelerated stress factors

The current hypothesis for coupling several stress is first to assume that there is no synergy between them. The total acceleration factor A of a test series is then the product of the individual acceleration factors obtained for each test. Therefore, relationship (7) has been proposed, where the global acceleration factor A is the product of all acceleration factor established for each stress [13].

$$A_n = a_1 \cdot a_2 \cdot \ldots \cdot a_n \quad (7)$$

Previous studies have shown that temperature, humidity and irradiation are the three most important stress factors for solar mirrors used in CSP installations [19]. Chemical stress like salt spray can be important too, but this stress factor is not specific to all of CSP installations. Considering our study, we can write the total acceleration factor (8) as the product of individual acceleration factor from temperature, humidity and irradiation.

$$A_{T+RH+I} = a_T \cdot a_{RH} \cdot a_I \quad (8)$$

In any case, the overall degradation may not follow the previous law, if synergistic factors exist. To take into account this, empirical relationships can be established to model the degradation that occurs during a test using all stress factors of interest. Concerning solar mirrors only two studies are reported:

The first model was developed by Jorgensen et al [28]. This model is based on Eyring's law, which requires an activation energy for the temperature *Ea* and an activation energy for the humidity (β). Several material dependent constants, *C* and *B*, are added. The effect of temperature T is weighted by a coefficient *n*. This model therefore inherently has the possibility of expressing a synergy between temperature and humidity, but the radiative stress is only taken into account by the I_{UV} value.

$$\Delta\rho = C \cdot I_{UV} \cdot T^{-n} \cdot e^{-\frac{Ea}{R \cdot T}} e^{RH\left(\beta + \frac{B}{T}\right)} \quad (9)$$

The second model has been proposed by Lee et al [29]. This model links the loss of specular reflectance with temperature, humidity and irradiation. Letters have the same correspondence than previously.

$$R_D = C \cdot I_{UV} \cdot e^{-\frac{Ea}{R \cdot T}} e^{B \cdot RH} \cdot t(s) \quad (10)$$

After studies of these different equations, we can conclude they must valid two hypotheses. Their authors formulate these two hypotheses implicitly. We clearly reformulate them:

1. Coupling hypothesis: Accelerating factors multiply each other without synergy. It is formulated in particular by equation (7).
2. Initialization hypothesis: It states that if a sample undergoes several accelerated tests, the order of the application of these tests is not important. This assumption is never explicitly stated and is already called into question in literature, for example with salt spray corrosion and by all the "frozen moisture" tests, i.e. lowering the sample to a temperature below 0°C with the presence of water. Concerning multi-stress with temperature, humidity and irradiation, we do not have found references witch mention an impact of the initialization.

2.3. Climate chambers for multiple stress factors

Artificial accelerated aging test is an efficient approach to assess the quality of solar reflectors and its degradation behavior over their life-time operation. It can be used to examine the impact of various ambient factors. Solar reflectors will be subjected in real environment, which includes solar irradiation, temperature, humidity, corrosion and sandstorm.

In order to study the influence of the three combined stress factors, temperature, relative humidity and irradiation, we conducted accelerated aging tests in three different chambers because no commercial unique equipment could produce the elevated level of these three stresses factors.

To reproduce elevated levels of UV radiation available at elevated outdoor desert climates, the testing conditions must be simulated and accelerated by climate chambers over a controlled and short laboratory test. Today the most common light sources are fluorescence or the so-called QUV, metal-halide mercury and xenon arc light. The most widely QUV accelerated aging test used for many years in various laboratories for quality testing and research experiments on reflectors components are UV light and humidity test according to the standard ISO 16474-3 [30] as presented in [31], [7] and [3]. It consists of several cycles composed of two steps. In the first step, the samples are exposed to UV radiation (λ = [290–400] nm) for 4 h at a temperature of T = (60 ± 3)°C. The UV lamps exhibit a peak at λ = 340 nm, with a radiation of 0.83 $W/m^{2}{\cdot}nm^{-1}$. Further, the mirror samples are submitted to 4 h of condensation (RH = 100% without irradiation) at T = (50 ± 3)°C. Therefore, one cycle lasts for 8 h. The power of the lamp is equivalent to that of the sun. Another standard used is ASTM G 53/96 [32], using fluorescent UVB lamp. The specimens are alternately exposed to UV light alone and to condensation alone in a repetitive cycle for at least 200 hours, using a test cycle of 8 h at 60°C with UV radiation alternating with 4 hours at 50°C with condensation.

We propose a new artificial test with alternation of dry phase and rain phase based on the standard ISO 16474-2 [33]. It consists of a constant irradiation at 65W/m² between 300 and 400 nm with a cycle of 27 min in dry environment followed by 3 min of rain. Temperature varies from 45°C during rain phase to 85°C during dry phase. The study of the paint coat degradation evidences that UV exposure is one of the most aggressive constraints for paint binder. But results show also a strong effect of liquid water on paint degradation and particularly on pigments loss and blistering phenomenon [17].

Only few manufactures can reproduce elevated levels of UV radiation test chamber in the world. It is a high technology and it is difficult to produce. These few manufactures are : Qualtech [34], Q-LAB [35] & ATLAS [36] from USA, Wewon [37] in China and SUGA [38] from Japan. However, the available level of irradiation and temperature is not sufficient for our experiment. A relevant review of J.W. Martin et al [24] on exposure of a polymeric material to high UV radiation fluxes for accelerating polymer photo-degradation shows the successful extrapolation results to in-service radiation flux levels. This review also discusses on the unavailability of commercial high radiant flux exposure equipment and, unanswered questions related to the effect of temperature and relative humidity on the photo-degradation of polymeric materials at high flux levels. The most accelerated UV test is carried out at CEA with a high level of UV-radiation in a chamber dedicated named UV-5X from BIA/AMC/AMTC. Six Solar Constant UV 2000 lamps (Hydrargyrum medium-arc iodide or HMI) allow a homogeneous controlled irradiation of 205 W/m² ± 15% between 300 and 400 nm (five times of solar ultraviolet conform to standard EN 61646). There is no standard for this test. The reflectors are also subjected to controlled temperature and UV radiation over different longer periods.

2.4. Purpose of this article

The aim of this article is to validate the actual models based on the coupling of several accelerated stress factors (see equations 8, 9, 10), such as temperature, humidity and UV irradiation. The goal is to perform an experimentation especially designed to test the main law actually proposed by the literature (equation 8). More specifically, we are going to test the two hypotheses actually used: the coupling hypothesis and the initialization hypothesis.

Such models are necessary for a better understanding of the degradation kinetics during time for several outside conditions. In addition, they are also necessary because experiments are very hard or impossible to be performed with three or more accelerated stress factors. The market does not actually propose environmental chambers which

can easily couple temperature, humidity and irradiation stresses. If our study shows that the coupling and the initialization hypothesis are true, it will be possible to study the interaction of several combined stress factors in one climatic chamber which is able to perform all these stresses. This could be advantageous in terms of investment for laboratories and companies. The samples chosen in this paper are silvered-glass CSP mirrors sensitive to three stress factors : temperature, humidity and UV irradiation [14], [39], [19]. Even if the subject is CSP mirrors, this study can be relevant also for the degradation and durability of PV, paints, plastic, building, or other applications where temperature, humidity and irradiation can have significant impacts.

3. Experimental

3.1. Accelerated aging plan

The test plan consists in combining three stress factors: temperature alone (T), temperature + humidity (T+HR) and temperature + UV (T+Irr) by alternating short, medium or long test times in each climatic chamber. Table 1 illustrates and synthesizes the test plan: in **blue** the temperature + humidity tests (marked T+HR), in **red** only the temperature tests (marked T) and in **green** irradiation and humidity tests (marked T+Irr). The effect of the first cyclical test will also be studied. Each sample will undergo a total test duration of 12 weeks.

- 4 weeks at a temperature of 95 °C.
- 4 weeks at a relative humidity of 85% and a temperature of 95°C.
- 4 weeks at 200W / m^2 UV irradiation and a mirror temperature of 95°C.

The total duration of 12 weeks (2016h) of testing will be divided into three groups:

- Short Cycle (abbreviated SC) of one week (168h).
- Average Cycle (abbreviated AC) of two weeks (336h).
- Long Cycle (abbreviated LC) of four weeks (672h).

Week n°12, each samples will have undergone the same total aging time, but with a different turnover (cycle time, SC or AC or LC). We have also studied the impact of the first stress mechanism in the aging process. At the end, we have 9 different conditions of tests, depending on the duration of the cycle (short, average or long) multiplied by three first stress encountered by the sample (T+HR, T, T+Irr). For each condition (e.g. Short Cycle, start with T+HR) we used a set of 3 identical samples from the same manufacturer for statistical reasons and in order to be more easy to replace in the case of destruction. In conclusion, we need 27 samples for the complete accelerated aging plan per manufacturer.

Week n°	n°1	n°2	n°3	n°4	n°5	n°6	n°7	n°8	n°9	n°10	n°11	n°12
Short Cycle	1st turnover = 3 weeks			2nd turnover = 3 weeks			3th turnover = 3 weeks			4th turnover = 3 weeks		
Start T+HR	T+HR	T+Irr	T	T+HR	T+Irr	T	T+HR	T+Irr	T	T+HR	T+Irr	T
Start T	T	T+HR	T+Irr	T	T+HR	T+Irr	T	T+HR	T+Irr	T	T+HR	T+Irr
Start T+Irr	T+Irr	T	T+HR	T+Irr	T	T+HR	T+Irr	T	T+HR	T+Irr	T	T+HR
Average Cycle	1st turnover = 6 weeks						2nd turnover = 6 weeks					
Start T+HR	T+HR		T+Irr		T		T+HR		T+Irr		T	
Start T	T		T+HR		T+Irr		T		T+HR		T+Irr	
Start T+Irr	T+Irr		T		T+HR		T+Irr		T		T+HR	
Long Cycle	1st turnover = 12 weeks											
Start T+HR	T+HR				T+Irr				T			
Start T	T				T+HR				T+Irr			
Start T+Irr	T+Irr				T				T+HR			

TABLE 1. Accelerated aging plan.

At the end of this protocol, the two hypotheses are tested:

- If the same degradation of samples from the same manufacturer occurred for all the three cycle durations: short, average or long, then the coupling hypothesis is true.
- If the first test encountered has no incidence on the degradation rate, then the initialization hypothesis is true.

3.2. Accelerated aging tests

In this study, all the samples are subjected to three accelerated aging tests, summarized in the Table 2.

Test	Manufacturer	Model	Parameter	Testing time
Temperature T	Vötsch	VTU60/60	T = 95°C	12 weeks
Humidity T+HR	Weiss	WKL100/40	T = 95°C & RH = 85%	12 weeks
Irradiation UV T+Irr	BIA Climatic AMC/AMTC	UV-5X	200W/m^2 T_{sample} = 95°C	12 weeks

TABLE 2. Summary of the accelerated aging tests

The constant temperature and humidity T+HR test consists in exposing the samples to a constant climate of 95 ± 2°C and 85 ± 5% of relative humidity. Samples are positioned in the chamber with an inclination of around 25° to the vertical, front side up. The irradiation UV-5X test consists in exposing the samples to a high UV radiation dose. The temperature inside the chamber is monitored at 88°C to obtain 95°C on the back side of the sample. The relative humidity is not controlled, but the UV-5X ensures a permanent air renewal. The UV-5X is heated by a heat pump, which creates warm and dry air. All aging tests were conducted during the summer 2019 at Le Bourget du Lac, France. The climate is hot and dry. In conclusion, even if the ambient humidity level remains uncontrolled, it is still acceptable. In any case, all samples were subjected to the condition and the same duration. In UV-5X, samples are placed in the chamber in front of the light source (HMI lamp + filter, 200 W/m² [300-400 nm]).

3.3. Characterizations

In this study, all the samples are measured by three different methods. Optical reflectance analysis is performed according to the actual SolarPACES reflectance measurement guideline [40]. Both spectral hemispherical reflectance and monochromatic specular reflectance are measured before and after the tests to characterize the total optical degradation. Degradation of paint have been studies by a colorimeter BYK Gloss [41], [42]. Equipment and methods for measuring reflectance of concentrating solar reflector materials in this study are based on bibliography [43], [44]. These characterizations are summarized in the Table 3.

Characterization	Instrument	Manufacturer	Model	Accessory	Measurement
Hemispherical Reflectance	Spectrophotometer	Perkin Elmer	Lambda 950	Integrating Sphere (Ø 150 mm)	$\rho_{\lambda,h}$*([280,2500],8°,h)*
Specular reflectance	15R-USB	D&S	-	-	$\rho_{\lambda,\varphi}$*(660nm,15°,12.5mrad)*
Colorimetry	Spectro-guide 45/0 gloss	BYK	-	-	CIE L*a*b, ΔE

TABLE 3. Summary of the measurement equipments

3.3.1. Hemispherical Reflectance measurement

Spectral hemispherical reflectance (noted $\rho_{\lambda,h}(\lambda,8°,h)$) is measured with a Perkin Elmer Lambda 950 spectrophotometer, with an integrating sphere of 150 mm diameter in the solar wavelength range [280 – 2500 nm] in 5 nm steps. Following ASTM Standard E903-82 [45], the solar-weighted hemispherical reflectance $\rho_{s,h}([280,2500],8°,h)$, is calculated thereafter, thanks to the equation below [46]. For simplification reason, we noted the solar-weighted hemispherical reflectance $\rho_{s,h}$ in this paper.

$$\rho_{s,h} = \rho_{s,h}([280,2500],8°,h) = \frac{\int_{280}^{2500} \rho_{\lambda,h}(\lambda,8°,h)\cdot G_b(\lambda)d\lambda}{\int_{280}^{2500} G_b(\lambda)d\lambda} \quad (11)$$

The solar-weighted hemispherical reflectance is the capacity of a surface to reflect the flux density (W/m^2) from the sun, depending of the sun power distribution. In our case the sun power distribution, noted $G_b(\lambda)$ is given by the ASTM G173-03 Direct and Circumsolar ratio [47], [48].

3.3.2. Specular Reflectance measurement

The monochromatic specular reflectance is measured with the portable D&S 15R-USB reflectometer to detect an eventual loss of reflectance of silver. It allows measuring the specular reflectance at 660 nm with an incident angle θ_i= 15° and a half acceptance angle φ = 12.5 mrad. This device is cited in the literature as a reference commercial product and can be compared to the Abengoa Condor SR 6.1 reflectometer [49]. Three different position points are measured on the samples and the mean value is calculated with standard deviation. In this paper the monochromatic specular reflectance measured with the D&S is noted $\rho_{\lambda,\varphi}$.

3.3.2. Color measurement

The color of the mirror backside is measured on a spectral range from 400 nm to 700 nm using a portable BYK spectro-guide 45/0 gloss colorimeter. The colorimetric model used is the CIE L*a*b developed in 1976 by the International Lighting Commission CIE [50]. Measured parameters are the luminance "*L*" and two parameters of chrominance "*a*" and "*b*" describing color respectively from red to green and from yellow to blue. The total color difference ΔE is a parameter calculated from the three measured values "*L*", "*a*" and "*b*" (12), "*ref*" values being the ones measured on the sample before aging.

$$\Delta \mathrm{E} = \sqrt{(L_{\mathrm{ref}} - L)^2 + (a_{\mathrm{ref}} - a)^2 + (b_{\mathrm{ref}} - b)^2} \tag{12}$$

Before characterization, samples are cleaned with demineralized water and wiped with optical paper to limit the risk of scratching the surface. To monitor optical deterioration, the specular reflectance is measured each week with the D&S 15R-USB reflectometer, and the color changes of the paint is measured with the BYK colorimeter. The characterizations calendar was as follow:

- Before and after tests every sample is characterized by all devices.
- At middle time (6 weeks, t= 1008h) samples from short (SC =1 week) and average cycle (AC = 2 weeks) have been characterized by hemispherical reflectance, three points per sample.
- At the end of every cycle (T, T+HR, T+Irr), each sample is characterized with D&S and colorimeter (three points per sample). That means that samples from short cycle group have been characterized 13 times, samples from average cycle group have been characterized 7 times and samples from long group have been characterized 4 times, as show in Table 1.

Despite of a very good measurement quality and low measurement uncertainty, we only perform hemispherical reflectance measurements before, at middle and at the end of test time.

3.4. Samples

The samples were four commercial silvered-glass mirrors of 70 mm x 70 mm size with a thickness of 1 mm for samples #1 and a thickness of 3 mm for samples #2, #3 and #4. Figure 1 illustrates for each sample the composition associated to a MEB picture from [38]. Because of the scale used, the nanometric thin layers of silver and copper are nearly invisible. Samples are presented in Figure 1 from #1 to #4, as follows:

1. Samples from manufacturer #1 are the specific ones for three different reasons. Firstly, the low iron glass thickness is reduced to 1 mm. Secondly, only two different paints are used (red and green). Finally, we do not have noted the presence of a thin copper layer between the silver and the red paint.
2. Samples from manufacturer #2 are composed of 3 mm of low iron glass and three different paints for back protection. Two metallic layers have been noted during characterization: a silver layer and a copper layer.
3. Samples from manufacturer #3 are composed of iron glass and three different paints. The solar reflectance is insured by a thin silver layer with a copper layer.
4. Samples from manufacturer #4 are composed of iron glass, silver, copper thin layer and three different paints.

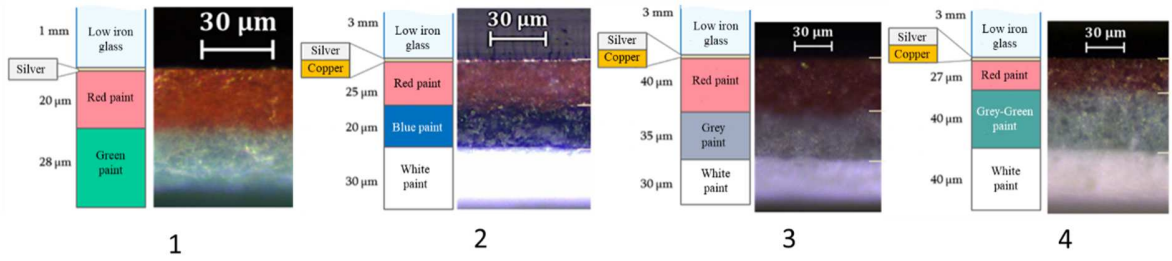

FIGURE 1. Samples presentation from manufacturers #1, #2, #3 and #4 [39].

The first important point is that paints can only be described in terms of color because the paint compositions are kept in secret by the manufacturer. In all cases the paint in contact of the metallic layers (copper for samples #2, #3, #4 and silver for samples#1) is the red paint. Expect samples #1, all manufacturers use a white paint for the last layers. The second point is that the total number of samples included in this study was 120. Indeed, we need 27 samples per manufacturer (3 samples per test, multiplied per 9) and 3 reference samples have been kept intact for comparison. This high number of samples required for this study was one of the main obstacles for more ambitious targets. Considering that constraint, theses samples have been chosen because they are the most commercially used. We are conscious that other types of mirror exist, particularly aluminum mirror, laminated mirror or polymeric mirror.

4. Results

4.1. Statistical analyses and aging detection

For this study, we need an accurate statistically test to detect aging differences between two samples, or two sample types. The aim is to conclude if two sets of measurements are statically different, according to their average, their range, the number of measures and by considering an alpha risk (noted α). The result of the bilateral range test (noted v) can show us if the measured deviation can be explained by a simple measurement of uncertainty [51]. For this test we need the average (noted m) and the range (max-min, noted w) of the two data set tested (here, sample n°1 and sample n°2). A data set can be just one sample, one small group of samples (ex: Short Cycle with T start from manufacturer #1) or a big group of samples (ex: Short Cycle from manufacturer #1). The equation for this test is:

$$v = \frac{|m_2 - m_1|}{w_1 + w_2} \tag{12}$$

After its calculation, the value v calculated must be compared to a reference v_{ref}, available in the abacuses of a statistical book. We note that v_{ref} is only a function of the number of measurement points for each sample.

- If $v > v_{ref}$: we can say, with the risk α of being wrong, that the two data sets n°1 and n°2 are statically different.
- If $v < v_{ref}$: no difference on the two data sets can be pointed out.

We have considered three different risk factors α=0.1; α=0.05 and α=0.01. For example, α=0.05 means that 5% of comparison will be positive, even if in reality no degradation exists. This false-positive value will be due to a statistical hazardous. It is important to note that the value v changes in function of the test conditions, the used manufacturers and the measurement devices. This statistical test allows us to conclude, to accept or to reject difference between two sample groups without personal interpretation. With a total number of 360 specular measurements on 30 samples of each manufacturer with the D&S, we can perform different statistic tests. Table 4 shows the data and the results for specular reflectance. We observe that samples for each manufacturer (from #1 to #4) have reflectance differences (solar or specular). We can perform the same calculation for hemispherical reflectance and colorimeter measurements. For additional information, we have added the mean (m_{pop}) and the standard deviation (σ_{pop}) of all the 30 samples. The values v are much higher than the values specified in the abacuses, even for the smallest risk of error (v_{ref} =0.187 for α=0.01 for 12 measurement points on both average). We

must considerate that small cut mirror samples (7 cm * 7 cm) from the same batch of a manufacturer are not strictly identical in term of reflectance, then, it is imperative to characterize all of them.

Type	m_{pop}	σ_{pop}	m_1	w_1	m_2	w_2	v_{cal}
Samples #1	0.9688	0.16%	0.9702	0.6%	0.9661	0.3%	0.4352
Samples #2	0.9599	0.10%	0.9612	0.2%	0.9586	0.3%	0.5167
Samples #3	0.9554	0.14%	0.9573	0.2%	0.9532	0.7%	0.4537
Samples #4	0.9624	0.20%	0.9653	0.3%	0.9578	0.8%	0.6742

TABLE 4. Comparison of two means of specular reflectance, performed in a sample test.

4.2. Initial characterizations

Before tests (at t=0h), three measurements were performed on each sample by rotating the sample 90° each time for hemispherical reflectance, at three different spots for colorimetry measurements and 12 measurements per sample were performed for monochromatic specular reflectance with D&S. The initial results are presented in the Table 5 below. Samples #1 (59.69) are different to the other ones (in the range of 94 to 95). This is due to the color of the external paint, green for samples #1 and white for samples #2 to #4.

	D&S		Spectrophotometer		Colorimeter	
	$\bar{\rho}_{\lambda,\varphi}$	$\sigma(\rho_{\lambda,\varphi})$	$\bar{\rho}_{S,h}$	$\sigma(\rho_{S,h})$	$\bar{E}_{col}$	$\sigma(E_{col})$
Sample #1	0.9688	0.16%	0.9542	0.21%	59.69	0.10%
Sample #2	0.9599	0.10%	0.9428	0.10%	94.34	0.09%
Sample #3	0.9554	0.14%	0.9361	0.28%	94.26	0.66%
Sample #4	0.9624	0.20%	0.9451	0.24%	95.10	0.13%

TABLE 5. Results of mean and standard deviation at t=0h for each manufacturer with the D&S ($\bar{\rho}_{\lambda,\varphi}$), Perkin Elmer spectrophotometer ($\bar{\rho}_{S,h}$) and the colorimeter ($\bar{E}_{col}$)

4.3. Comparison of the rotation cycles - coupling hypothesis

The following Figures 2.A & 3.B compare the degradation loss of specular reflectance ($\Delta\rho_{\lambda,\varphi}$, Figure 2.A) and the solar-weighted hemispherical reflectance ($\Delta\rho_{s,h}$, Figure 2.B). All the figures are in function of the cycle duration: the mean results between the different types of stresses (T or T+HR or T+Irr) for the same cycle duration (SC, AC or LC). Each figure is presented as a bar graph in function of their cycle duration. For each comparison, we have added the lower α risk used. As an example, for samples #1, with α=0.01, maximum specular reflectance loss is equal to 1.72% and is observed for the long cycle (dashed bar). The specular reflectance losses observed between the short (dark grey) and medium cycles (light grey) are too close to conclude. For samples #2 and #3, none of the duration cycles show different reflectance losses but a significant loss of 3 % and 12 % respectively for samples #2 and #3. The high amplitude between cycles prevents conclusion. This high amplitude is perfectly explained by the effect of the starting cycle, as we will explain in the next section. Concerning sample #4, it can be shown at (α=0.05) that the medium and short cycles caused more degradation than the long cycle.

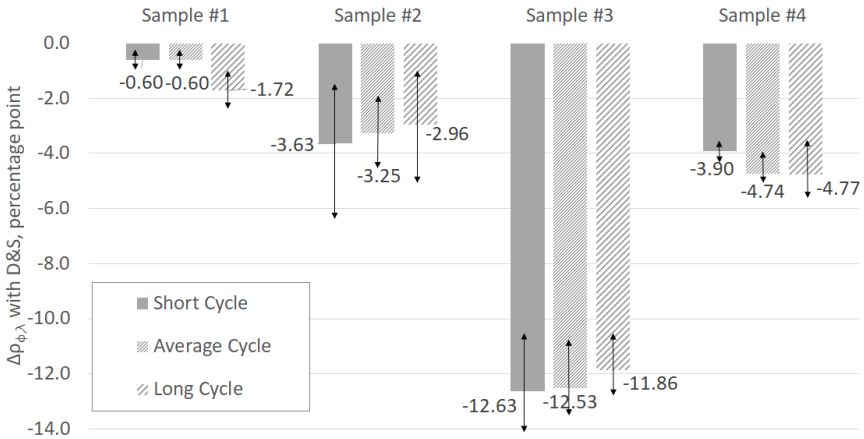

FIGURE 2.A. Specular reflectance ($\Delta\rho_{\lambda,\varphi}$) losses for samples #1 to #4 in function of their cycle duration

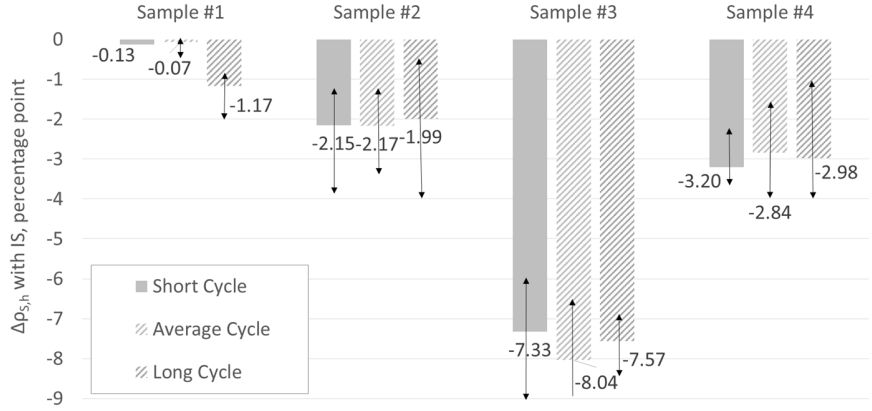

FIGURE 2.B. Solar-weighted hemispherical reflectance ($\Delta\rho_{S,h}$) losses for samples #1 to #4 in function of their cycle duration

Regarding to the solar-weighted hemispherical reflectance, it is easy to conclude that the long cycle is the most aggressive test (α=0.01) for samples from manufacturer #1. The too short difference of reflectance between the short and medium cycles does not allow to conclude. For samples #2 to #4, the low difference of reflectance between the cycle durations does not allow to conclude according to the presentation of Figure 2.B. As seen before, the high amplitude of each measurement can be explained by the effect of the first aging test. By analyzing the impact of the cycle duration of the same first aging test, it is possible to conclude several times with a lowest risk of (α=0.05 or less) that the cycle duration has an impact. The colorimetric degradation (ΔE) for samples #1 to #4 is proposed in the Table 6.

For each sample, we compared different cycle durations for the same first aging test (T+HR or T or T+Irr) using the method described in paragraph 4.2. We count the number of each positive comparison (if $v > v_{ref}$; means the two data are statically different) according to the risk α. Table 6 shows the summary of all the four sample types, after tests. For example, for a comparison of the specular reflectance according to α=0.05, the value "2" for Short cycles vs average cycles beginning by T+HR means that 2 samples group of the four types are different. First, we need to remember that before tests, all values are equal to zero, except for colorimetry (not all samples from the same batch are comparable with each other). The effect of cycle duration seems to be closely related to the effect of the first stress. With a first test T+HR, a total of 9 over 48 differences of reflectance degradation in function of cycle duration are observed. For a start in T, cycle duration seems to have no effect on the total loss at t=2016h of specular or solar reflectance. The first test occurred undoubtedly has a non-negligible effect. We observe a total of 23 over 48 comparisons attesting that the samples are not comparable each other (α=0.05). For all three cases (beginning by T+HR, T or T+Irr), colorimetry results show almost a systematic effect of cycle durations on the ageing of the paints

on the back of the mirrors. The last line 'Total' shows the percentage of the number of positive comparison (in case the hypothesis is wrong) in the total number of comparison. This percentage must be reported to the alpha risk: the more the difference is; the more the hypothesis can be rejected.

		Specular reflectance		**Solar weighted hemispherical reflectance**		**Colorimeter**	
		$\alpha = 0.05$	α=0.01	$\alpha = 0.05$	α=0.01	$\alpha = 0.05$	α=0.01
Start T+HR	Short vs Average	2	0	3	0	2	2
	Short vs Long	1	0	1	0	4	3
	Average vs Long	1	0	1	0	4	3
Start T	Short vs Average	1	0	0	0	4	3
	Short vs Long	0	0	0	0	3	3
	Average vs Long	0	0	0	0	3	3
Start T+Irr	Short vs Average	1	2	2	2	4	2
	Short vs Long	2	1	1	1	3	3
	Average vs Long	3	1	3	1	1	1
Total		*44%*	*31%*	*56%*	*56%*	*89%*	*83%*

TABLE 6. Number of positive comparisons for four samples for specular, solar-weighted hemispherical reflectance and colorimeter

4.4. Comparison of the order test effect - initialization hypothesis

The following figures present the degradation loss for specular reflectance ($\Delta\rho_{\lambda,\varphi}$ Figure 3.A), solar-weighted reflectance (Δρs,h, Figure 3.B) and the discoloration (ΔE, Figure 3.C) of the paints. All figures are bar charts in function of the first stress encountered by the samples. Stress of temperature and humidity (T+HR: 95°C and 85% RH) are represented with blue bars, temperature alone (T: 95°C) is in red bars and temperature and irradiation (T+Irr 95°C + 200 W/m2 of UV) in green bars. We have averaged the results between the different types of cycle duration (short: SC, average: AC and long: LC). For each positive comparison, we have added the lowest α risk used in the Figures description. Concerning the specular reflectance losses, we observe two different behaviors. Firstly, for the samples from manufacturer #1.The loss of reflectance observed between a start by T+HR and T+Irr of $\Delta\rho_{\lambda,\varphi}$ = -0.65% allows to conclude (α=0.05) that the start by T+Irr is more deleterious. The difference is too small for the two others. Secondly, for mirrors of manufacturers #2 to #4, the T+HR start is clearly the most deleterious on the specular reflectance. For mirrors #2 and #3 the risk is lower than α =0.01 if we compare a T+HR start vs T alone. For these samples, we can conclude that the starting test with T alone is less damaging than the starting test with T+Irr, considering a risk α=0.05 for samples #2 and a risk α=0.01 for samples #3. For mirrors #4, we can only conclude with certainty that starting with a T+HR cycle is more penalizing than starting with a T+Irr cycle with a risk of α=0.1.

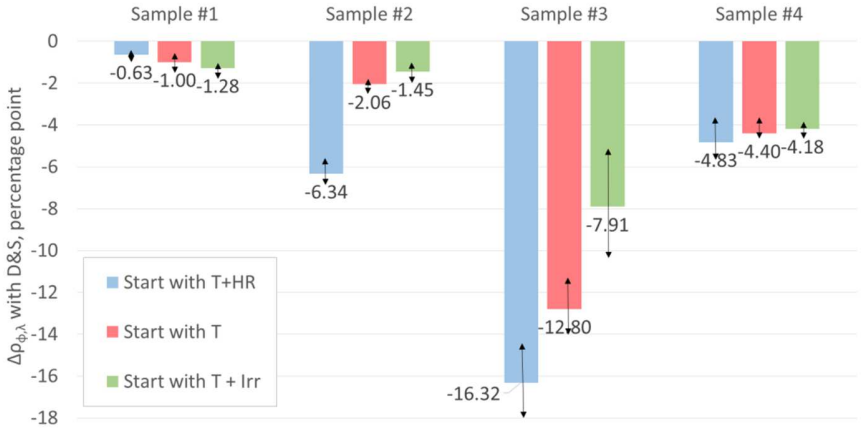

FIGURE 3.A. Specular reflectance ($\Delta\rho_{\lambda,\varphi}$) losses for samples #1 to #4 in function of the initial stress encountered

For solar-weighted hemispherical reflectance, the same conclusion can be drawn as previously. For samples #1, we are sure that starting by the aging process with a T+Irr stress (green column) is more deleterious (with α=0.01) than with T+HR (blue column) and then with T (α=0.05). The difference between T+HR and T+Irr is not sufficient to conclude. Samples #2 and #3 have the opposite effect as previously. The difference between each column is sufficient to conclude that an onset of ageing by a T+HR cycle induces much more degradation than with a first stress in T+Irr (α< 0.01). For samples #4 the very small difference between a T+HR or T start does not allow to conclude ($\Delta\rho_{s,h}$ < 0.1%). This near equality is surely due to uncertainties and the two departures seem to have the same effects. T+Irr is certainly less deleterious ($\Delta\rho_{s,h}$ = -1.7%) than the other two stresses with high confidence (α = 0.01).

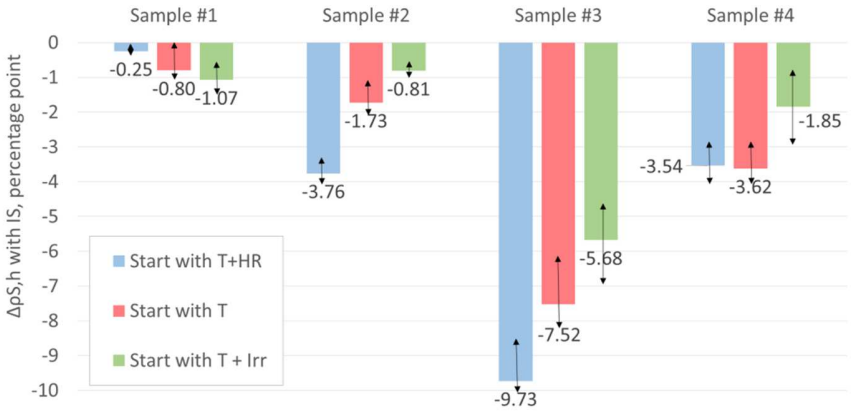

FIGURE 3.B. Solar-weighted hemispherical reflectance ($\Delta\rho_{s,h}$) losses for samples #1 to #4 in function of the initial stress encountered

Figure 3.C shows the loss of ΔE colorimetry of the paints according to the first test. For samples #1 the analysis in colorimetry is difficult, because the green paint of these mirrors has been strongly damaged. 12 samples out of the 27 show a visible deterioration, with a loss of material. All the mirrors starting with a T+Irr test had their paint deteriorated, sometimes significantly, where more than 50% of the surface of the back of the mirror is no longer covered with paint. This leaves the silver layer exposed. Conversely, all the samples which started with T+HR aging have their paint intact. On the remaining areas of paint, the difference in color ΔE between the three starts allow us to conclude for all cases with α=0.01. We notice that the start in T+HR is the most deleterious, followed by the T alone and then by the T+Irr test, in this order. We can then conclude that T+HR > T > T+Irr, concerning only the color of the remaining paint. This conclusion is the opposite of the one formulated for reflectance losses where T+Irr > T > T+HR. By trying to take into account the quantity of paint remaining, we will retain this conclusion. Concerning samples #2 to #4, we can conclude that α=0.01 so that the greatest loss of color is observed for a start in T+Irr. Temperature seems to offer the lowest stress level for paints, but this is not statistically proven. The small difference between T+HR and T was more deleterious than the T+Irr cycle, but with α=0.05 do not allow to separate these two stress levels.

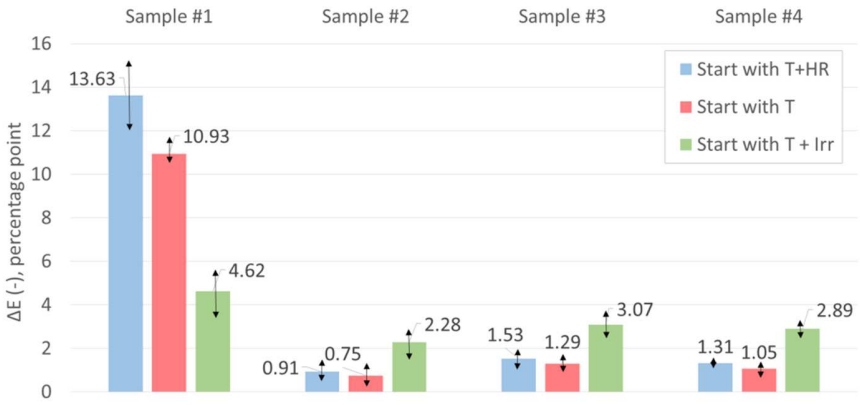

FIGURE 3.C. Colorimetric degradation (*ΔE*) losses for samples #1 to #4 in function of the initial stress encountered

Table 7 provides a summary as previously (see Table 6 for explanation). The effect of the first stress encountered by a mirror on optical reflectance degradation (specular or solar) or colorimetry of paints (ΔE) is really important. 27 comparisons of the specular reflectance (measured with D&S) reveal that for the same manufacturer two groups of samples with the same cycle duration are not comparable, because of the influence of the first stress encountered. The last line 'Total' shows the percentage of the number of positive comparison (in case the hypothesis is wrong) in the total number of comparison. This percentage must be reported to the alpha risk: the more the difference is; the more the hypothesis can be rejected.

		Specular reflectance		**solar-weighted hemispherical reflectance**		**Colorimeter**	
		α=0.05	α=0.01	α=0.05	α=0.01	α=0.05	α=0.01
Short Cycle	T+HR vs T	1	1	1	1	2	1
	T+HR vs T+Irr	2	2	2	2	4	4
	T vs T+Irr	2	1	3	3	4	4
Average Cycle	T+HR vs T	2	1	3	3	3	2
	T+HR vs T+Irr	1	1	3	3	4	4
	T vs T+Irr	0	0	1	1	4	4
Long Cycle	T+HR vs T	1	1	1	1	3	3
	T+HR vs T+Irr	4	3	3	3	4	4
	T vs T+Irr	3	1	3	3	4	4
Total	-	*31%*	*11%*	*22%*	*11%*	*78%*	*64%*

TABLE 7. Number of positive comparisons for four samples for specular, solar-weighted hemispherical reflectance and colorimeter

4.5. Conclusion

Even if the stated hypothesis is true, a statistical test is not 100% reliable. This is why we talk about accepting a risk α (see §4.1). Knowing that, we can compare the number of positive comparisons attesting the reality of a different degradation rate (here, the stated hypothesis) to the natural chance, for each sample and for each measuring device. For recall, a positive comparison mean that the stated hypothesis is wrong. By logical construction, it is not possible to test if a hypothesis is true: we can only fail several time to prove that the hypothesis is incorrect. In our case, a positive comparison show that there is a difference between two samples, while the tested hypothesis predict the opposite (no difference). Table 8 shows an overview of Table 6 (comparison of the rotation cycles - coupling hypothesis) and Table 7 (comparison of the order test effect - initialization hypothesis).

Specular reflectance | **solar-weighted** | **Colorimeter**

			hemispherical reflectance			
	α=0.05	α=0.01	α = 0.05	α=0.01	α = 0.05	α=0.01
Risk of false positive	5%	1%	5%	1%	5%	1%
Coupling hypothesis	31%	11%	22%	11%	78%	64%
Ratio (X/α)	6	11	4	11	16	64
Initialisation hypothesis	44%	31%	56%	56%	89%	83%
Ratio (X/α)	9	31	11	56	18	83

TABLE 8. Part of positive comparisons, for each sample and device according to the α risk, concerning both hypotheses

If the two hypothesis were true, we would observe a number of positive comparison close to α risk, due to a statistical hazardous (false positive). For example, with α=0.05, 5% of comparisons will be positive even when the hypothesis is true. We must compare the percentage of false positive (alpha) to the percentage of positive comparison observed here. For both hypotheses, we observed that this percentage is several times higher than α. The ratio of the numbers of time where each hypotheses can be reject to alpha is strictly superior to 1, for every case. In conclusion, it is reasonable to highlight that both hypotheses, coupling and initialization, are false. The global degradation of solar mirrors (reflectance and paints) is very sensitive to the order of the different stresses and the duration of the cycles. We synthesize:

1. The two hypotheses formulated above are wrong. The accelerating factors multiply each other with a synergy and the order of the application of the environmental stresses has a significant role.
2. Each mirror has a different behavior compared to the experimental plan.
3. It is impossible to substitute a three-stresse climate chambers (T+Irr+HR) by several climate chambers with two stresses. The influence of the cycle duration and the initialization are too strong.

5. Discussion

5.1. Main degradations observed

All degradation mechanisms cannot be fully described in this paper and more details would be found in another future article. We would remind that the aim of this paper is not to reproduce the natural degradation mechanism. Indeed, the goal was to observe the impacts of the different cycles where the conditions selected were extreme. As an example, the conditions as T+HR at T = 95°C & RH = 85% for the T+HR stress test must be used with care because the degradation rate is significant and the degradation mechanisms can be different from outside.
Currently, we have not been able to establish a solid link between the mirrors test conditions and degradations (reflective side or paint). We have no accurate correlation between the loss of reflectance (specular or solar) and the loss of colorimetry of the paintings.

Briefly, we have observed two types of degradation on the samples of manufacturers #1 and #4. An example is shown in Figure 4. The paint of sample #1 is degraded. It is drawn away from the mirror back and falls as a fine dust. The operator has an important role here: mirrors with fast cycles (1-week rotation) have undergone more manipulations than the others. During a change of climate chamber, it is possible to remove large amounts of paint just by touching the mirror. At t=2016h, around 46 % of the sample from manufacturers #1 had degraded paint, either partially or almost completely. The first degradation seems to appear either after a T+HR test or after a T+Irr test. We observed that some degradations do not progress during time. There is also a role of luck: samples from the same group are not all affected by corrosion. The dark green square is a zone protected by a scotch tape used to monitor the mirror temperature.
The reflective face of samples #4 is covered with a kind of veil from the first stress in T+HR. Visually, the haze seems to be located between the glass and the silver layer. This induces a decrease of a few percentage in specular and solar-weighted hemispherical reflectance. The veil seems to be static and do not progress with the following passages. Externally the paint shows intact.

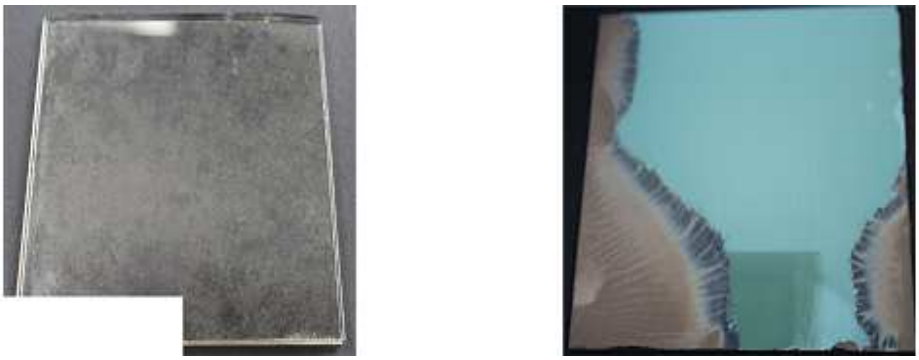

FIGURE 4 : Left : Reflective face of sample #4 at t=2016h (short rotation, start with T). Right : paint side on sample #1, after the same conditions than previously.

5.2. Advantages for T+Irr starting condition

One of the most surprising results of these tests concerns the difference in reflectance losses between mirrors starting with a temperature and irradiation test (T+Irr). Except for samples #1, the effect is proved for mirrors from manufacturers #2, #3 and #4 (see Figure 3.A and Figure 3.B). Firstly, several cases should be studied. For example, the difference observed may be due to a particular effect of the T+Irr from T or T+HR cycles. Secondly, the "protective" effect of UV or curing could be considered. Unfortunately, we have not studied other cycle alternations (in particular T+Irr→T+HR→T). Therefore, we cannot exclude this hypothesis. Moreover, we can add:

- Different placements in the UV-5X climate chamber are ignored. The number of rotations implies a "shuffling", especially with the mirrors of short cycle. They were moved several times and replaced in UV-5X climate chamber, in different places.

- Just by chance. Let us imagine that each set has 9 mirrors more resistant than the others, out of 27 mirrors tested. It would be statistically unlikely that these best 9 mirrors would all be randomly assigned to the batch starting with T+Irr and not to the others.

- The effect of solarization could also play a role here, in which transmittance of solar glass improves a little bit due to the influence of UV radiation. For that we should compare the transmittance spectra of samples at t=0h with the transmittance spectra after irradiation. We assume that probably in some spectral regions, the glass transparence will be increased after aging. This effect in the glass could lead to erroneous conclusions regarding the silver layer, particularly if iron ions are present in the glass. Unfortunately, we are not able to process these experiments now. We can only compare the spectral hemispherical reflectance of sample #3 (samples most affected by preventive irradiation) before and after ageing (t=2016h, complete cycle), according to two different initialization (T+HR strongly degraded and T+Irr less degraded), here presented in Figure 5. We observe that the main difference is between 250-1000 nm. In the NIR spectral area (up to 2 µm), we observe that aged mirrors (green and red curve) are more reflective than an intact mirror (blue curve), suggesting a modification in the glass or in the silver layer.

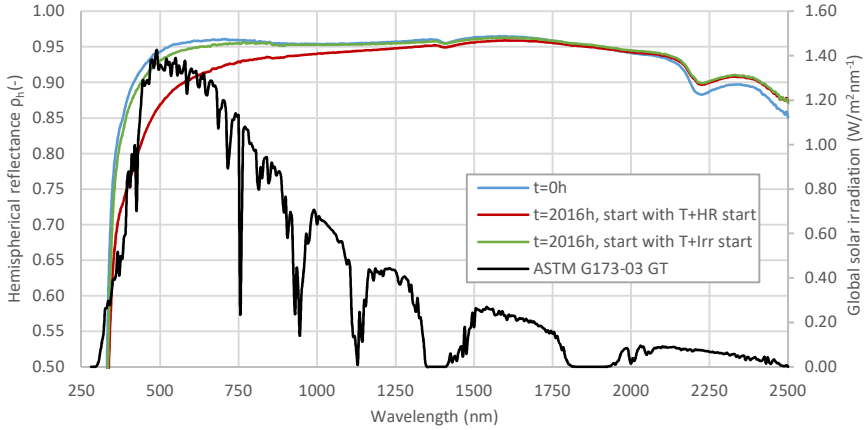

FIGURE 5. Spectral hemispherical reflectance $\rho_{\lambda,h}$ of sample #3 at t=0 and t=2016 for long cycle and two different initialization.

In conclusion, we are suspicious but we can even argue that it would be possible that prior UV irradiation would be beneficial for the mirror. We need to prospect this preventive irradiation with additional tests and characterizations. It is a safe bet that the difference is chemical, probably in terms of paintings. Our first clue is to study the resistance of paints to moist heat. The irradiation has probably modified their chemical compositions or rendered the paint layers non-permeable to water.

5.3. Weibull distribution

The Weilbull equation is used in durability field to analyze experimental data and to give a predictive scenario of reflectance losses during time. Several bibliographic sources confirmed a good correlation between the Weibull equation and the behavior of the solar mirrors under accelerated aging tests with one or two stress factors (T, or T+HR or T+Irr). Figure 6 shows the D&S reflectance losses measured from samples with a short rotation time (1 week) as a function of time from the beginning t=0h to the end of test t=2016h. We have selected the manufacturer #3 samples because the reflectance losses ($\Delta\rho_{\lambda,\varphi}$) are more significant compared to the other samples, in the range of 0 to -15%. This high reflectance loss compared to error uncertainty due to D&S makes the data more usable. We have selected only samples with a short duration time because theses samples are characterized every weeks, provided to us more points. In conclusion, we have more data to fit the Weibull curves with 12 points.

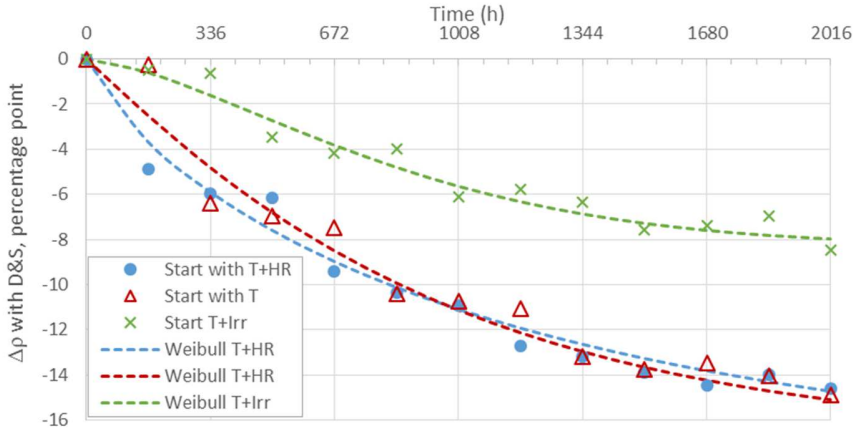

FIGURE 6. Weibull distribution of $\rho_{\lambda,\varphi}$ for manufacturer #3 mirrors, aging with 12 short cycles (168h)

These results confirm that several stress factors such a rotation between T, T+HR and T+Irr can be modeled with the Weibull distribution, in the case of short cycle. The absolute deviation is 0.1% for samples with a T+HR start, 0.2% for samples with T start and 0.4% for samples with T+Irr start. The impact of the initialization stress is clearly visible. Despite the same ageing time, mirrors starting with the T+Irr are less degraded than the two other groups.

6. Conclusions

In this study, we have studied the coupling of temperature, humidity and UV irradiation stresses on solar mirror degradations. For this purpose, we have chosen 4 different manufacturers of solar mirrors to provide a total of 120 samples. These samples have been split into 9 different groups to experiment the impact turnover (short and long average) and the initialization condition (first stress with the humidity or temperature or irradiation climate chamber). During 12 weeks (2016h) of accelerated ageing, we have performed multiple optical characterizations in specular and solar reflectances in addition to colorimetry measurement of the paints. At the end, statistic tests have been used to compare samples. If each sample was subjected to the same duration of each stress (4 weeks in each climate chamber), the first stress (temperature, humidity and irradiation) and the turnover (1, 2 or 3 weeks) were different.

Firstly, we conclude the effect of the first stress encountered by a solar mirror as a very important effect on its durability. This case is demonstrated for all mirrors, with a very low risk of false results. It appears that the first environmental conditions of the life of the mirror are decisive on its lifespan. Likewise, the effect of the first test has

a significant impact on corrosion. Secondly, the duration of the cycles has an impact on the loss of reflectance. However, not all the mirrors are affected. In addition, we have proved that it is not possible to substitute the combination of three stress factors by several climate chambers with one or two stresses. If we really want to study the impact of three simultaneous stress factors, we absolutely need an appropriate climate chamber. One of the most surprising results of multi-factor aging tests is the lifespan longer of mirrors that underwent firstly radiation stress. We have shown that this difference is not in coincidence, and that the drop of reflectance is not negligible. The hypothesis of "protective" effect of UV or curing the paints with the UV radiation could be considered in a future paper with sequence of tests cycles T+Irr→T+HR→T. It is therefore necessary to investigate this phenomenon based on a better understanding of the degradation mechanisms occurring. Finally, it would also be interested to analyze more finely the materials and the paintings to understand the chemical degradation mechanisms according to the different stress factors in comparison with the optical characterization performances.

Acknowledgments

The research leading to this article has received funding from French national funding from Agence Nationale de la Recherche on the program Investissements d'Avenir (n°ANR-11-EQPX-0014).

References

[1] O. Achkari, A. El Fadar, Latest developments on TES and CSP technologies – Energy and environmental issues, applications and research trends, Appl. Therm. Eng. 167 (2020) 114806. https://doi.org/10.1016/j.applthermaleng.2019.114806.

[2] H.L. Zhang, J. Baeyens, J. Degrève, G. Cacères, Concentrated solar power plants: Review and design methodology, Renew. Sustain. Energy Rev. 22 (2013) 466–481. https://doi.org/10.1016/j.rser.2013.01.032.

[3] O. Behar, A. Khellaf, K. Mohammedi, A review of studies on central receiver solar thermal power plants, Renew. Sustain. Energy Rev. 23 (2013) 12–39. https://doi.org/10.1016/j.rser.2013.02.017.

[4] P. Kurup, C.S. Turchi, Parabolic Trough Collector Cost Update for the System Advisor Model (SAM), 2015. http://www.nrel.gov/docs/fy16osti/65228.pdf.

[5] C.S. Power, Technology Roadmap Concentrating Solar Power, Current. 5 (2010) 1–52. https://doi.org/10.1787/9789264088139-en.

[6] C. Turchi, M. Mehos, C.K. Ho, G.J. Kolb, Current and future costs for parabolic trough and power tower systems in the US market, Renew. Energy. (2010) 11. http://www.nrel.gov/docs/fy11osti/49303.pdf.

[7] F. Sutter, A. Fernandez-García, J. Wette, P. Heller, Comparison and evaluation of accelerated aging tests for reflectors, Energy Procedia. 49 (2014) 1718–1727. https://doi.org/10.1016/j.egypro.2014.03.181.

[8] M. Mazzucato, G. Semieniuk, Financing renewable energy: Who is financing what and why it matters, Technol. Forecast. Soc. Change. 127 (2018) 8–22. https://doi.org/10.1016/j.techfore.2017.05.021.

[9] J.J.C.S. Santos, J.C.E. Palacio, A.M.M. Reyes, M. Carvalho, A.J.R. Freire, M.A. Barone, Concentrating Solar Power, Adv. Renew. Energies Power Technol. 1 (2018) 373–402. https://doi.org/10.1016/B978-0-12-812959-3.00012-5.

[10] T. Craig, Parabolic Trough Reference Plant for Cost Modeling with the Solar Advisor Model (SAM), NREL/TP-550-47605. Natl. Renew. Energy Lab. (NREL), Golden, CO. (2010) 112. http://www.nrel.gov/docs/fy10osti/47605.pdf.

[11] L.A. Escobar, W.Q. Meeker, A review of accelerated test models, Stat. Sci. 21 (2006) 552–577. https://doi.org/10.1214/088342306000000321.

[12] W.B. Nelson, Accelerated Testing: Statistical Models, Test Plans, and Data Analysis (Wiley Series in Probability and Statistics), (2004) 624. http://www.amazon.com/Accelerated-Testing-Statistical-Probability-Statistics/dp/0471697362.

[13] M. Kohl, B. Carlsson, G. Jorgensen, A.W. Czanderna, Performance and Durability Assessment, Optical Ma, 2004.

[14] C. Avenel, O. Raccurt, J.L. Gardette, S. Therias, Review of accelerated ageing test modelling and its application to solar mirrors, Sol. Energy Mater. Sol. Cells. 186 (2018) 29–41. https://doi.org/10.1016/j.solmat.2018.06.024.

[15] F. Dia, N. Mbengue, O.N. Sarr, M. Diagne, O.A. Niasse, A. Dieye, M. Niang, B. Ba, C. Sene, Model Associated with the Study of the Degradation Based on the Accelerated Test: A Literature Review, Open J. Appl. Sci. 06 (2016) 49–63. https://doi.org/10.4236/ojapps.2016.61006.

[16] S. Arrhenius, Über die Reaktionsgeschwindigkeit bei der Inversion von Rohrzucker durch Säuren, Zeitschrift Für Phys. Chemie. 4U (2017). https://doi.org/10.1515/zpch-1889-0416.
[17] R. Girard, C. Delord, A. Disdier, O. Raccurt, Critical Constraints Responsible to Solar Glass Mirror Degradation, Energy Procedia. 69 (2015) 1519–1528. https://doi.org/10.1016/j.egypro.2015.03.103.
[18] A.W. Czanderna, P. Schissel, Specularity and stability of silvered polymers, Sol. Energy Mater. 14 (1986) 341–356. https://doi.org/10.1016/0165-1633(86)90057-2.
[19] C. Avenel, O. Raccurt, J.-L. Gardette, S. Therias, Accelerated aging test modeling applied to solar mirrors, Npj Mater. Degrad. 3 (2019) 1–14. https://doi.org/10.1038/s41529-019-0089-y.
[20] C. Avenel, J.L. Gardette, S. Therias, A. Disdier, O. Raccurt, Accelerated aging test of solar mirrors: Comparison of different UV chambers, AIP Conf. Proc. 1850 (2017). https://doi.org/10.1063/1.4984495.
[21] S. Dugaria, A. Padovan, V. Sabatelli, D. Del Col, Assessment of estimation methods of DNI resource in solar concentrating systems, Sol. Energy. 121 (2015) 103–115. https://doi.org/10.1016/j.solener.2015.07.043.
[22] K.Schwarschild, On the effect of intermittent exposure on bromide of silver gelatine, (1899).
[23] K.Schwarschild, On the deviation from the law of reciprocity for bromide of silver gelatine, (1899).
[24] J.W. Martin, J.W. Chin, T. Nguyen, Reciprocity law experiments in polymeric photodegradation: A critical review, Prog. Org. Coatings. 47 (2003) 292–311. https://doi.org/10.1016/j.porgcoat.2003.08.002.
[25] D.J. Klinger, Humidity acceleration factor for plastic packaged electronic devices, 7 (1991).
[26] K.M. Striny, A.W. Schelling, Reliability Evaluation of Aluminum-Metallized MOS Dynamic RAM's in Plastic Packages in High Humidity and Temperature Environments, IEEE Trans. Components, Hybrids, Manuf. Technol. 4 (1981) 476–481. https://doi.org/10.1109/TCHMT.1981.1135819.
[27] D.S. Peck, Comprehensive model for humidity testing correlation, (1970) 44–50.
[28] G.J. Jorgensen, H.-M. Kim, T. Wendelin, Durability studies of solar reflector materials exposed to environmental stresses.pdf, Knowl. Creat. Diffus. Util. (1997) 20–54. https://doi.org/10.1081/E-EEE2-120046011.
[29] J. Lee, Lifetime Prediction for Degradation of Solar Mirrors using Step-Stress Accelerated Testing, (2011).
[30] ISO, Paints and varnishes - Methods of exposure to laboratory light sources - Part 3: Fluorescent UV lamps, 16474-3. (n.d.).
[31] A. Fernández-García, L. Martínez-Arcos, F. Sutter, J. Wette, F. Sallaberry, R. Erice, T. Diamantino, M.J. Carvalho, O. Raccurt, A.C. Pescheux, G. Imbuluzqueta, M. Machado, Accelerated aging test of solar reflectors according to the new AENOR standard - Results of a round Robin test, AIP Conf. Proc. 2033 (2018). https://doi.org/10.1063/1.5067231.
[32] ASTM G53-96 Practice for Operating Light- and Water-Exposure Apparatus (Fluorescent UV-Condensation Type) for Exposure of Nonmetallic Materials (Withdrawn 2000), ASTM International, West Conshohocken, PA, 1996.
[33] ISO, Peintures et vernis - Méthodes d'exposition à des sources lumineuses de laboratoire - Partie 1 : Lampes à arc au Xénon, 2014., 16474-2, NF EN. (n.d.).
[34] Q. Compagnie, Qualtech UV Weathering Test Chamber, (n.d.). https://www.qualtechproductsindustry.com/products/climatic-testing-instruments/weathering-equipments (accessed January 28, 2020).
[35] Q-LAB, QUV ® Accelerated Weathering Testers, (2011) 1–12.
[36] Atlas, UV Test-Fluorescent/UV, 2020.
[37] WeWon, WeWon UV test Chambers, (n.d.). https://www.wewontech.com/uv-test-chambers/ (accessed January 28, 2018).
[38] SUGA, 2020.
[39] C. Avenel, Durabilité des miroirs pour l ' énergie solaire à concentration : étude des modes de vieillissement, Université de Savoie Mont-Blanc, 2018.
[40] S. Meyen, M. Montecchi, C. Kennedy, G. Zhu, Parameters and method to evaluate the solar reflectance properties of reflector materials for concentrating solar power technology, SolarPACES. (2013).
[41] E. Schütz, F. Berger, R. Barillon, P. Audebert, A. Chambaudet, Behaviour of painted mirrors during exposure tests to salt spray, Appl. Surf. Sci. 120 (1997) 106–118. https://doi.org/10.1016/S0169-4332(97)00219-5.
[42] E. Schütz, F. Berger, O. Dirckx, A. Chambaudet, Study of degradation mechanisms of a paint coating during an artificial aging test, Polym. Degrad. Stab. 65 (1999) 123–130. https://doi.org/10.1016/S0141-3910(98)00227-4.

[43] A. Fernández-García, F. Sutter, L. Martínez-Arcos, C. Sansom, F. Wolfertstetter, C. Delord, Equipment and methods for measuring reflectance of concentrating solar reflector materials, Sol. Energy Mater. Sol. Cells. 167 (2017) 28–52. https://doi.org/10.1016/j.solmat.2017.03.036.
[44] F. Buendia-Martinez, A. Fernandez-Garcia, F. Sutter, L. Martinez-Arcos, T.J. Reche-Navarro, A. Garcia-Segura, L. Valenzuela, Uncertainty study of reflectance measurements for concentrating solar reflectors, IEEE Trans. Instrum. Meas. 69 (2020) 1–1. https://doi.org/10.1109/tim.2020.2975387.
[45] ASTM, ASTM E903-82. Standard Test Method for Solar Absorptance, Reflectance, and Transmittance of Materials Using Integrating Spheres., (2012).
[46] S. Meyen, M. Montecchi, C. Kennedy, G. Zhu, Guidelines: parameters and method to evaluate the solar reflectance properties of reflector materials for concentrating solar power technology, SolarPACES. (2013). https://doi.org/elib.dlr.de/84546.
[47] ASTM G173–03 Standard Tables for Reference Solar Spectral Irradiances: Direct Normal and Hemispherical on 37° Tilted Surface, ASTM Stand. (2003). https://doi.org/https://doi.org/10.1039/C3EE43825B.
[48] C.A. Gueymard, D. Myers, K. Emery, Proposed reference irradiance spectra for solar energy systems testing, Sol. Energy. 73 (2002) 443–467. https://doi.org/10.1016/S0038-092X(03)00005-7.
[49] C. Sansom, A. Fernández-García, P. King, F. Sutter, A. Garcia Segura, Reflectometer comparison for assessment of back-silvered glass solar mirrors, Sol. Energy. 155 (2017) 496–505. https://doi.org/10.1016/j.solener.2017.06.053.
[50] G. Wyszecki, W. Stiles, Colour Science: Concepts and Methods, Quantitative Data and Formulas, 2nd ed., New York, 2020. https://doi.org/10.1080/713818072.
[51] V.E. Johnson, Revised standards for statistical evidence, Proc. Natl. Acad. Sci. U. S. A. 110 (2013) 19313–19317. https://doi.org/10.1073/pnas.1313476110.